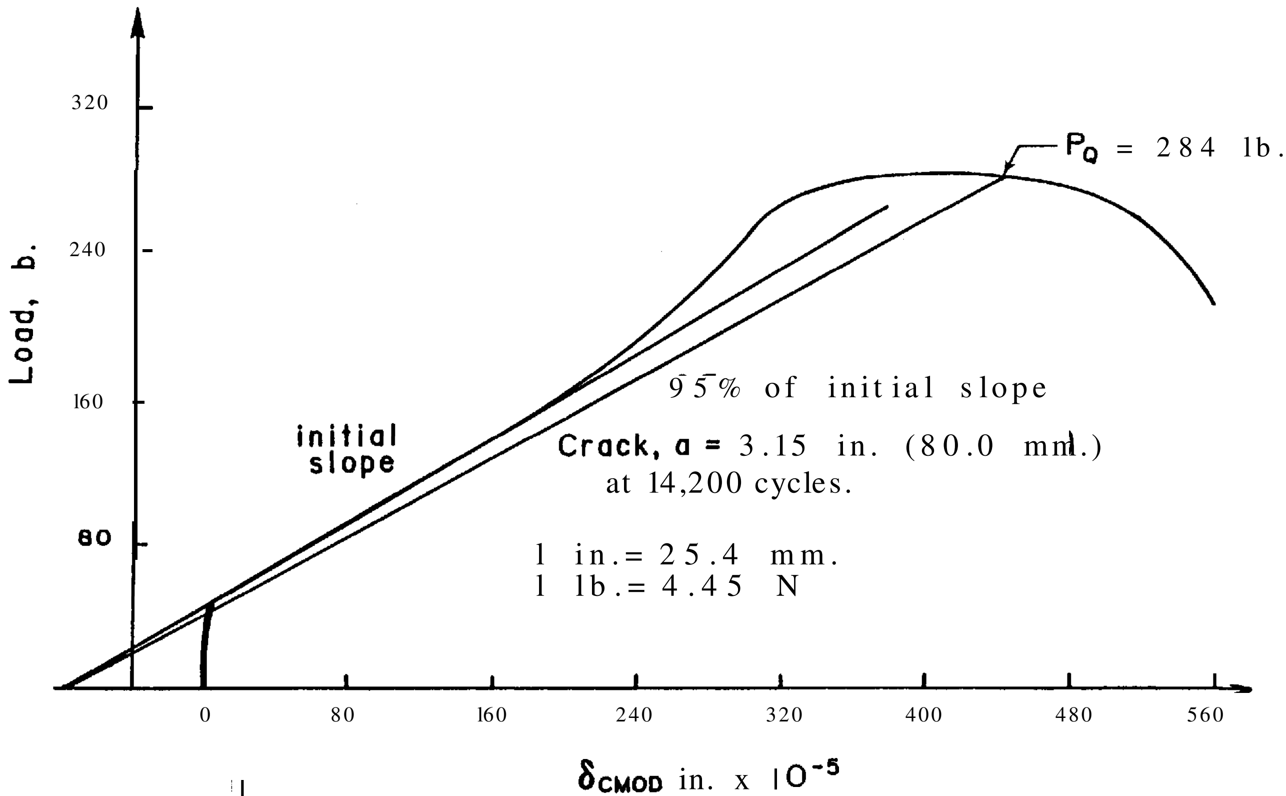

Fig.6.3 Load versus δ_{CMOD}

1. Cut a small starter notch at midspan.

2. Using a ramping function and strain control, load the beam beyond P_u, grow a crack and then remove the load. Subsequently, plot P versus δ_{CMOD} using a maximum load $\leq$ 1/3 the maximum load associated with the crack.

3. Introduce the dye and cycle the load to work the dye into the cracked surface. The beam must be loaded with the crack proceeding from the top surface downward. The load must be greater than that needed to overcome crack closure stresses and must be less than about 1/3 of P_u.

4. Dry the dyed surface and load the beam to failure. Plot P and δ_{CMOD}. The initial slope after crack closure is overcome gives the initial compliance C_i.

5. After failure, measure the dyed surface area. The initial crack length is

$$a_i = (\text{area of dyed surface})/b \tag{6.4}$$

Typical dyed surfaces are shown in Fig. 6.4.

6. Repeat steps 1-5 for different crack depths and establish calibration curves relating C_i and a_i, P_u and a_i. The latter relationship allows one to obtain an estimate of the crack length associated with any load on the softening part of the load-displacement plot.

7. At the point on the unloading plot corresponding to the onset of unstable crack growth – taken to be at 0.95 P_u determine the extended crack length a_i from the $P_u - a_i$ plot (step 6). The extended length must not be greater than a_e/d = 0.65. Using 0.95 P_u and a_e compute K_{Ic} from

$$K_{Ic} = F(s, d, b, a_e, 0.95P_u) \tag{6.5}$$

The validity of the procedure to estimate the extended crack length a_e may be argued by referring to a load-unload-reload diagram (Fig. 6.5). The objective is to determine the crack length at some point on the softening branch – say point C (which may be any point). If the actual unloading trace is available, the unloading compliance C_u can readily be measured and used with a compliance calibration curve to determine the extended crack length a_e. Alternatively, the $P_u - a_i$ relationship may be used where the load at point C is used for P_u. In constructing the $P_u - a_i$ curve, it is noted from Fig. 6.5 that an approximation exists in that P_u and a_i imply the use of the slope of line OB instead of the actual line OA. The error in determining the crack length from this approximation was determined to be less than 6% with a coefficient of variation of 8.5% (62 samples) (Swartz and Refai, 1989).

The results obtained by using this method on 8 in. and 12 in. deep beams with $a_e/d \leq$ 0.65 show K_{Ic} to be invariant with respect to the crack length and beam size, with a coefficient

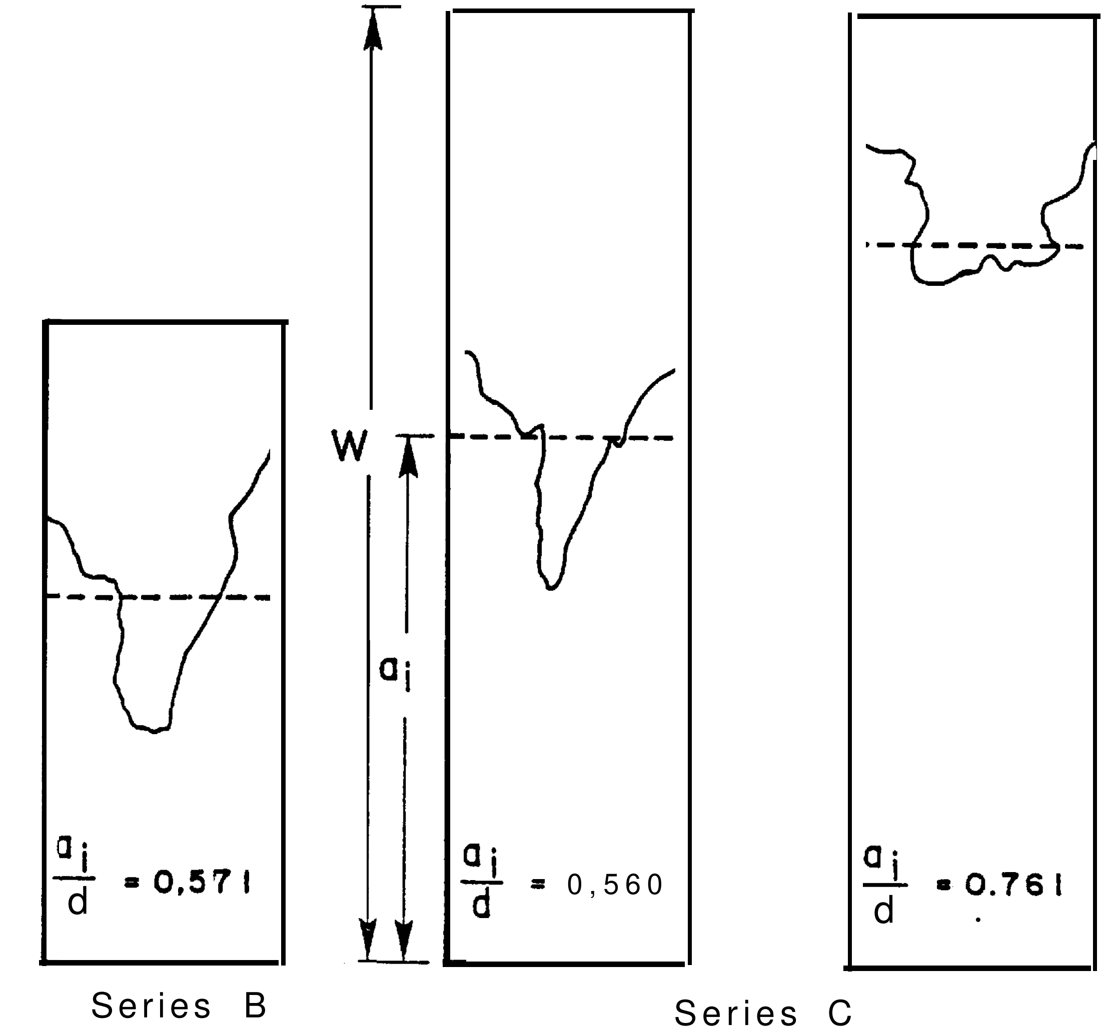

Fig.6.4 Dyed Cracked Surfaces

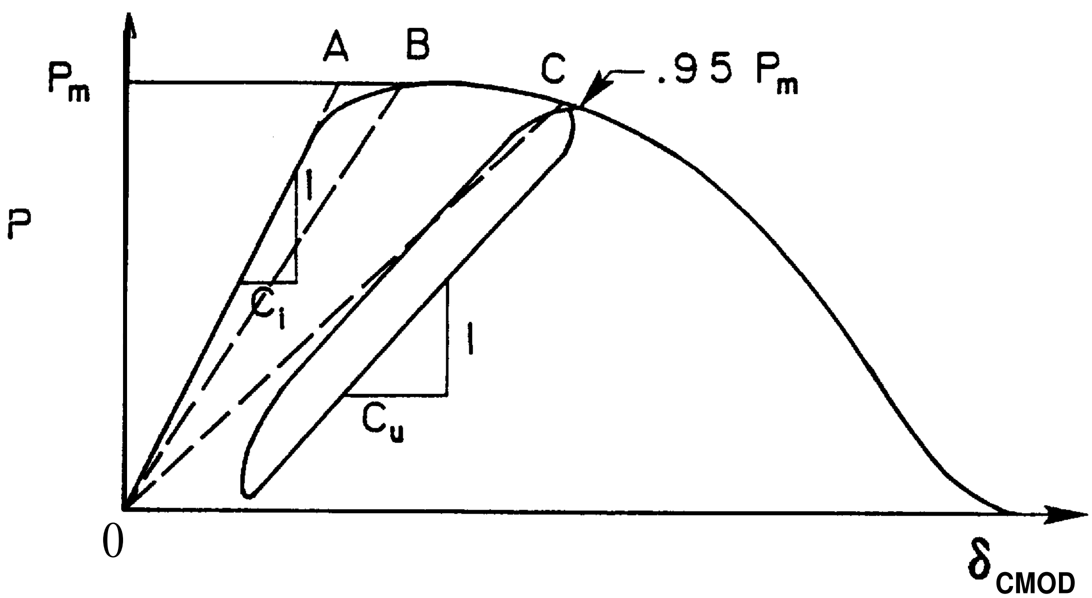

Fig.6.5 Load versus δ_{CMOD} with Reload at 0.95 P_u

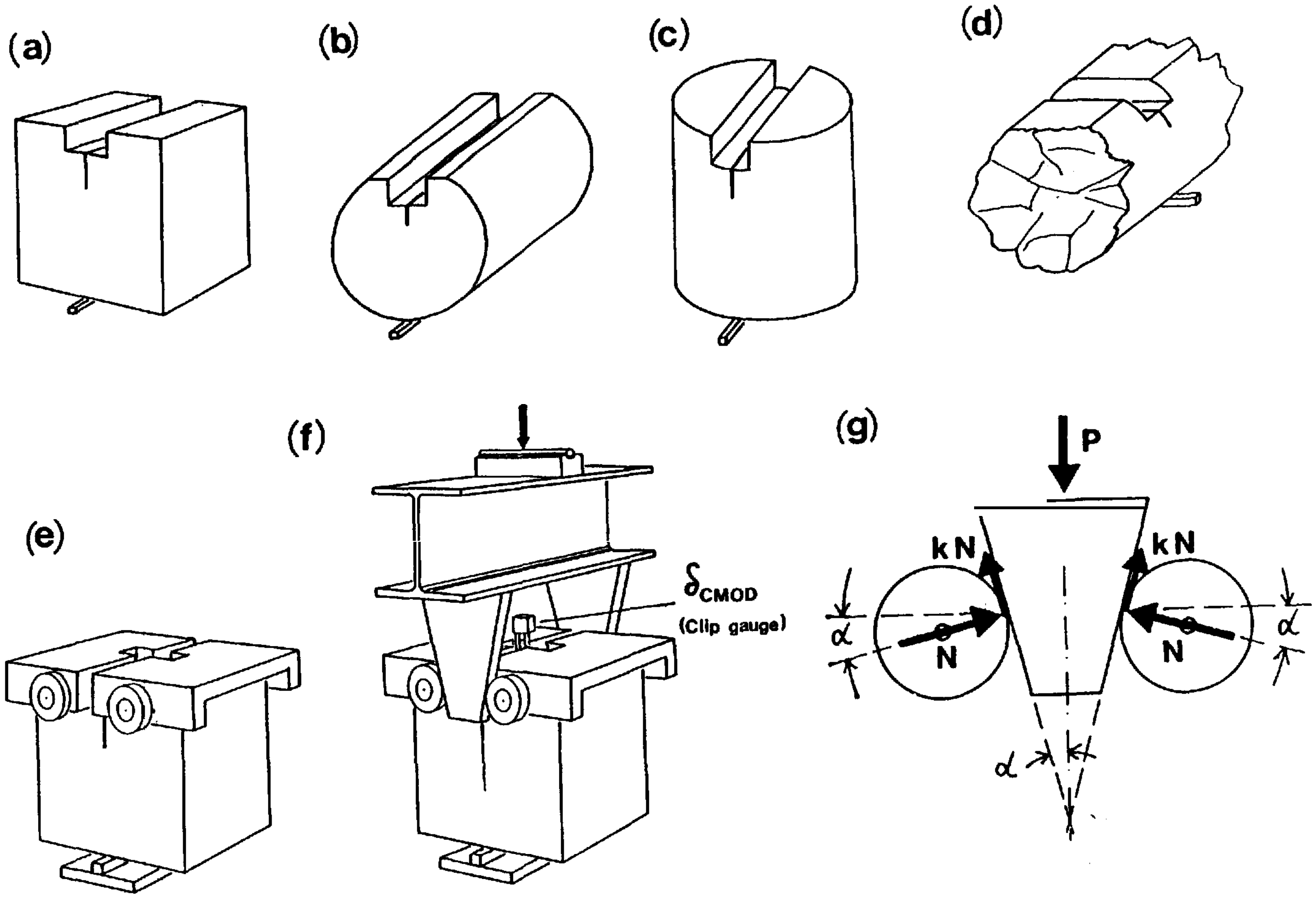

Fig.6.6 (a) Wedge-Splitting Specimen Shape, (b-c) Alternative Shapes, (e-f) Loading Devices, (g) Forces Acting on the Wedge.

of variation of 5.5% (N = 19, 8 in. beams) and 3.5% (N = 19, 12 in. beams) (Refai and Swartz, 1988; Swartz and Refai, 1989).

6.1.4 Effect of Friction

An advantage of notched beam tests is that friction effect is small. To explain this effect, let ηd be the distance from the bottom face (Fig. 6.1) to the point on the crack plane such that an axial force passing through this point would cause no deflection of the beam; obviously $a_0/d < \eta < 1$ (typically $\eta = 0.75$). If the horizontal friction forces acting at the beam supports are denoted as F, the bending moment at midspan needed to cause crack propagation is $M = (P/2)(S/2) - F\eta d$ where S = span, P = applied load, $F = kP/2$ and k is the coefficient of friction. Denoting $P_0 = 4M/S$, which represents the force needed to cause the crack to propagate if there were no friction ($k = 0$) one gets $P_0 = P - \Delta P_f$ where P = measured applied force and (according to Bazant):

$$\Delta P_f = \frac{2\eta d}{S} kP$$

This represents the portion of the applied force needed to overcome the friction. The larger the S/d ratio, the smaller is ΔP_f. For $\eta = 0.75$ and $k = 0.005$ for roller bearings (manufacturers give an upper value of $k = 0.01$) and for $S/d = 2.5$ (used by Bazant and Pfeiffer, 1987), $\Delta P_f = 0.003P$. Thus, we see that the notched beam tests are relatively insensitive to friction, which is their advantage compared to some other tests (as pointed out by Planas and Elices, 1988b).

6.2 Wedge-Splitting Test

Another useful test for fracture of concrete is the wedge-splitting test (Fig. 6.6). It is similar to the compact tension test used for metals. Wedge splitting tests were studied for concrete by Hillemier and Hilsdorf (1977) and the present shape of the test specimen, characterized by a starter notch and a guiding groove which can be either moulded or sawn, was proposed by Linsbauer and Tschegg (1986). The test was subsequently refined by Bruhwiler (1988), and Bruhwiler and Wittmann (1989) who conducted (at the Swiss Federal Institute of Technology) over 300 such tests on normal concrete, dam concrete and other cementitious materials. Very large wedge splitting specimens, of sizes up to 1.5 m (5 ft.), have recently been tested by Saouma, Broz, Bruhwiler and Boggs (1989) at the University of Colorado, to study the size effect in dam concrete.

Fig. 6.6 (a-d) shows various possible wedge-splitting specimen shapes. Specimen (Fig. 6.6c) requires either a deep notch or a longitudinal groove on both sides, in order to prevent shear failure of one of the cantilevers. Fig. 6.6 (e,f) illustrates the method of testing. The assembly of two wedges is pressed between two low-friction roller or needle bearings (on each side) which develop a pair of forces N that tend to split the specimen (Fig. 6.6g). The wedge assembly is loaded in a statically determinate manner so that each wedge receives the same load. The dimensions of the notch and the groove must be chosen so that the crack propagates symmetrically.

During the test, the splitting force N (Fig. 6.6g) must be measured with sufficient accuracy. The crack mouth opening displacement δ_{CMOD} is measured by a transducer or a clip gage (Fig. 6.6f) which should be attached at the level of the splitting forces, in which case δ – CMOD represents the load-point displacement δ_{LPD} associated with the horizontal component of the splitting force N. The test is controlled by δ_{CMOD} in a closed-loop servo-hydraulic testing machine. However, a stable test can also be performed under actuator stroke control or under crosshead displacement control using conventional testing machines. In that case, the appropriate notch length necessary to ensure stability must be identified by considering the interaction between testing machine stiffness, specimen stiffness and material properties (Brühwiler, 1988; Brühwiler and Wittmann, 1989).

The advantages of the wedge splitting test are as follows:

1) The specimens are compact and light, since the ratio of fracture area to the specimen volume is larger than for other tests (e.g., 5.2-times larger than that for the three-point-bend test according to RILEM, 1985). This is especially useful for the study of size effect, since larger fracture areas can be obtained with smaller specimen weight. Due to lesser weight, larger specimens are easier to handle, and there is a lesser risk of breaking them during handling.

2) The cubical or cylindrical specimens (Fig. 6.6 a-c) can be easily cast at the construction site using the same molds as for strength tests, and the cylindrical shapes (Fig. 6.6 b-d) can also be obtained from drilled cores from existing structures.

3) The use of wedges for inducing the load increases the stiffness of the test set-up and thus enhances stability of the test, making it possible to conduct the test even in a machine that is not very stiff.

4) the effect of selfweight is negligible in contrast to notched beam tests (where the bending moment due to own weight can be over 50% of the total bending moment).

On the other hand, it must be noted that the wedge loading has also a disadvantage as it intensifies frictional effects. Let P = applied vertical load, N = specimen reactions needed to propagate the cracks which are normal to the wedge surface inclined by angle a (Fig. 6.6g), and k = friction coefficient of the bearings. Then, the equilibrium condition of vertical forces acting on the wedge yields P = $2(N \sin \alpha + kN \cos \alpha) = P_o(1 + k \cot \alpha)$, where $P_o = 2N \sin\alpha$ is the force needed to propagate the crack if there were no friction (k = 0). Since $k \cot\alpha \ll 1$, we have $P_0 \simeq P/(1 + k\cot\alpha) = P(1 - k\cot\alpha)$ or $P + o = P - \Delta P_f$ where (according to Bažant):

$$\Delta P_f = PK \cot \alpha \tag{6.6}$$

P is the measured load and ΔP_f represents the portion of the load needed to overcome the friction. If $\alpha < 45°, \Delta P_f$ is larger than kP, which means that frictional effects are enhanced by the wedge loading.

For the typical wedge angle $\alpha = 15°, \Delta P_f = 3.73kP$. The manufacturers of roller bearings give k-values ranging from 0.001 to 0.005 (and guarantee 0.01 as the limit). Assuming $k = 0.005, \Delta P_f = 0.019P$. This frictional effect is significant and is about 6-times larger than for the short notched beams of Bazant and Pfeiffer (1987), and about 20-times larger than for the longer notched beams recommended by RILEM, for the same value of k (see Sec. 6.1.4.). This disadvantage of the wedge splitting test is surmountable, and frictional effects can be reduced by (1) attaching hardened steel inserts along the inclined wedge surface, (2) using needle bearings, and (3) carefully polishing the wedge surface as shown by Hillemeier and Hilsdorf (1977) who experimentally determined a K-value = 0.00031 for their wedge loading set-up with needle bearings.

If the value of k is nearly constant and well reproducible, one may introduce the correction ΔP_f in the analysis. However, since the value of friction coefficient is often quite uncertain, it is better to measure the splitting force N directly by instrumenting the wedges and the shafts that carry the bearings with strain gages.

The foregoing analysis shows that a very small wedge angle α is unfavorable from the viewpoint of friction. On the other hand, the smaller the angle, the stiffer is the specimen-machine assembly. The angle $\alpha = 15°$ is a reasonable compromise.

Also, a large wedge angle ($\alpha > 30°$) is undesirable because it leads to a significant normal stress parallel to the crack plane in the fracture process zone. The presence of such stresses may affect the softening curve for the fracture process zone, as described by Eq. 3.9. The area under the softening curve is then not longer equal to the fracture energy, G_f; nor is the area under the load-displacement curve.

The apparent fracture toughness, K_{Ic} is obtained by the same method as described in Section 6.1 for notched beam tests. The effective crack length, which accounts for the fracture process zone, is determined by the compliance method, based on finite element calibration. For that purpose, unload-reload cycles are performed during the test. Other methods such as the evaluation of fracture energy from the area under the load-displacement diagram and the size effect method are applicable, as described in the sequel.

6.3. Work-of-Fracture Method (RILEM, Hillerborg)

This method, which was originally developed for ceramics (Nakayama, 1965; Tattersall and Tappin, 1966) is the first method of testing for fracture properties of concrete to be proposed as a standard (RILEM, 1985). The basis for applying this method to concrete was developed by Hillerborg and his co-workers (Hillerborg, 1985b). Their method uses the "fictitious crack" concept (Hillerborg et al., 1976; Hillerborg, 1980; Petersson, 1981) (Fig. 6.7) implicitly and thus is not an LEFM method.

In order to contrast this with LEFM on the basis of energy parameters, recall that the critical energy release rate G_{Ic} is the energy required per unit crack extension in a material in which there is no process zone, that is, all the energy is surface energy and no energy is dissipated away from the crack tip. In fact, a process zone does exist and therefore the total energy of fracture includes all the energy dissipated per unit propagation distance of the fracture process zone as a whole. This is called the fracture energy G_f (Fig. 6.7).

Conceptually, the method can be applied to a variety of test specimen geometries but the proposed standard uses a beam specimen loaded in three point bending with a central

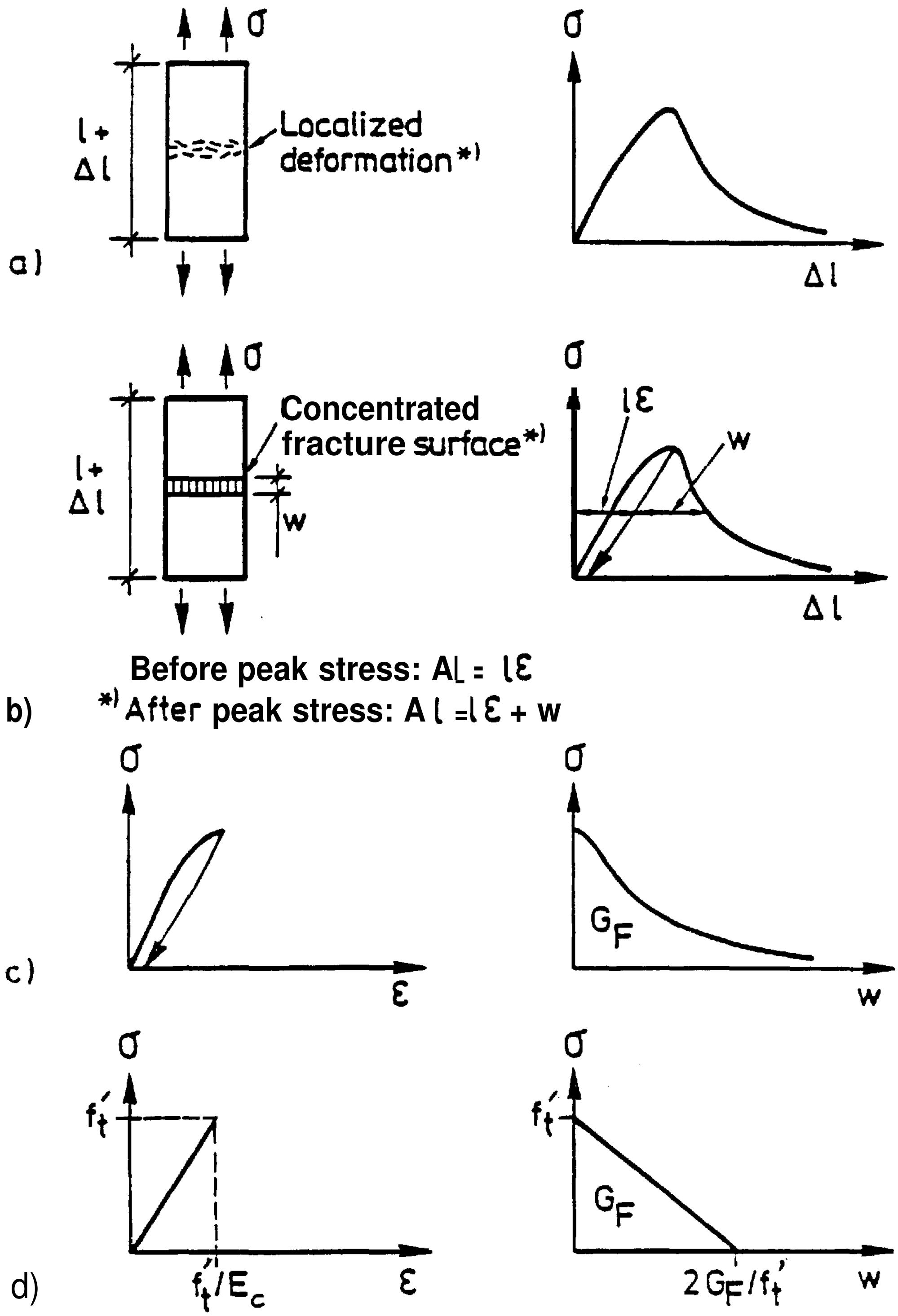

Fig.6.7 Fictitious Crack Model Description of Tensile Fracture

edge notch (Fig. 6.la). Complete details of the proposed standard are given in the RILEM Recommendation (1985) and are not repeated here. Briefly, the test procedure consists of the following steps.

1. The beam proportions are selected in relation to maximum aggregate size. The minimum depth d is approximately six times the size of the aggregate. The ratios of S/ d vary from 8 to 4. See Table 6.1. The beam specimen is notched to a depth a_0/d= 0.5.

2. The vertical load-point deflection of the beam (called δ_{LPD} in Fig. 6.1a) is to be measured and plotted continuously along with the applied load P. The resulting trace is shown in Fig. 6.8.

3. The test is to be conducted in a manner to produce stable crack growth. If closed-loop testing is used then strain control should be selected. If a closed-loop system is not available, then a stiff testing machine is required (stiffness recommendations are given in RILEM, 1985.)

4. The fracture energy is calculated as

$$G_f^R = \frac{W_0 + mg\delta_0}{A_{lig}} \tag{6.7}$$

in which W_0 = area under $P - \delta_{LPD}$ curve up to δ_0; δ_0 = displacement when P returns to 0; mg = $(m_1 + 2m_2)g$ and $m_1 g$ = beam weight between supports, $m_2 g$ = weight of fixtures which is carried by the beam; and A_{lig} = original, uncracked ligament area = $b(d - a_0)$.

This formula is valid if the movement of load and δ_{LPD} are downward. If the beam is tested "on its side" so that the applied load P is normal to the beam's self weight vector, then the term $mg\delta_0$ is neglected. Also, if the dead weight is otherwise compensated, this term is neglected.

Further, if the movements of load and δ_{LPD} are upward - thus opposing the self weight vector - then it is shown that (Swartz and Yap, 1988)

$$G_f^R = \frac{W_0 - \frac{1}{2}mg\delta_0}{A_{lig}} \tag{6.8}$$

in which δ_0 = displacement at the point on the unload portion of the plot when P = $(m_1/2 + m_2)g$.

Eqs. 6.6 and 6.7 were derived by Swartz and Yap (1988). The self weight term may be quite significant, especially if young concrete is being tested or the specimen is large.

Extensive round-robin tests from 14 laboratories incorporating about 700 beams were reported by Hillerborg (1985c). With regard to variation of results within a given tests series, the coefficient of variation ranged from about 2.5% to 25% with most results around 10 to 15%. It was noted that "... the sensitivity of the strength of a structure with regard to changes in G_f^R is normally less than 1/ 3 of the sensitivity with regard to changes in normal

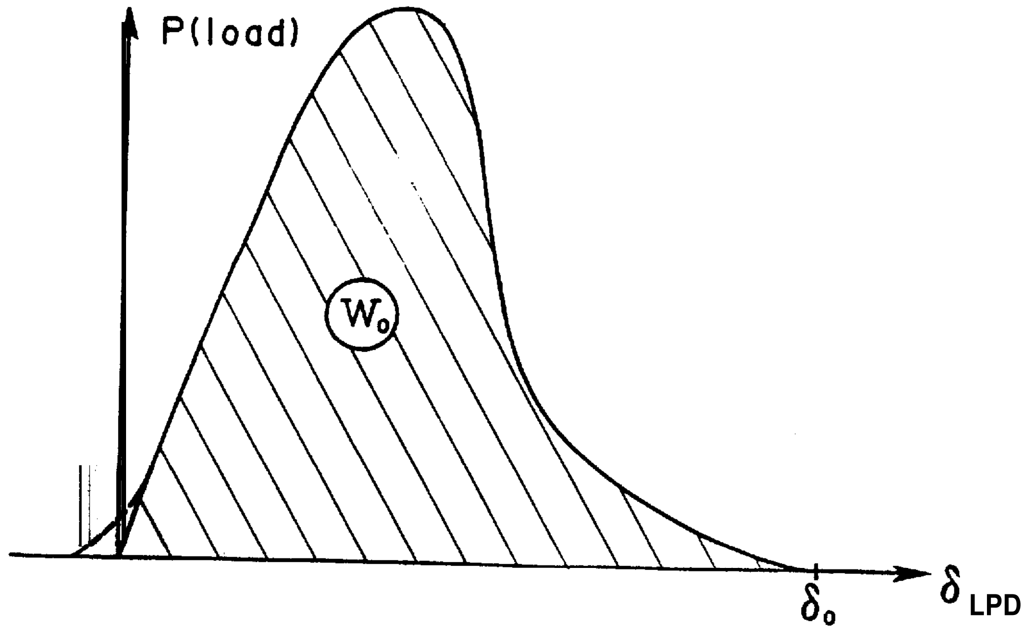

Fig.6.8 Load Versus δ_{LPD}

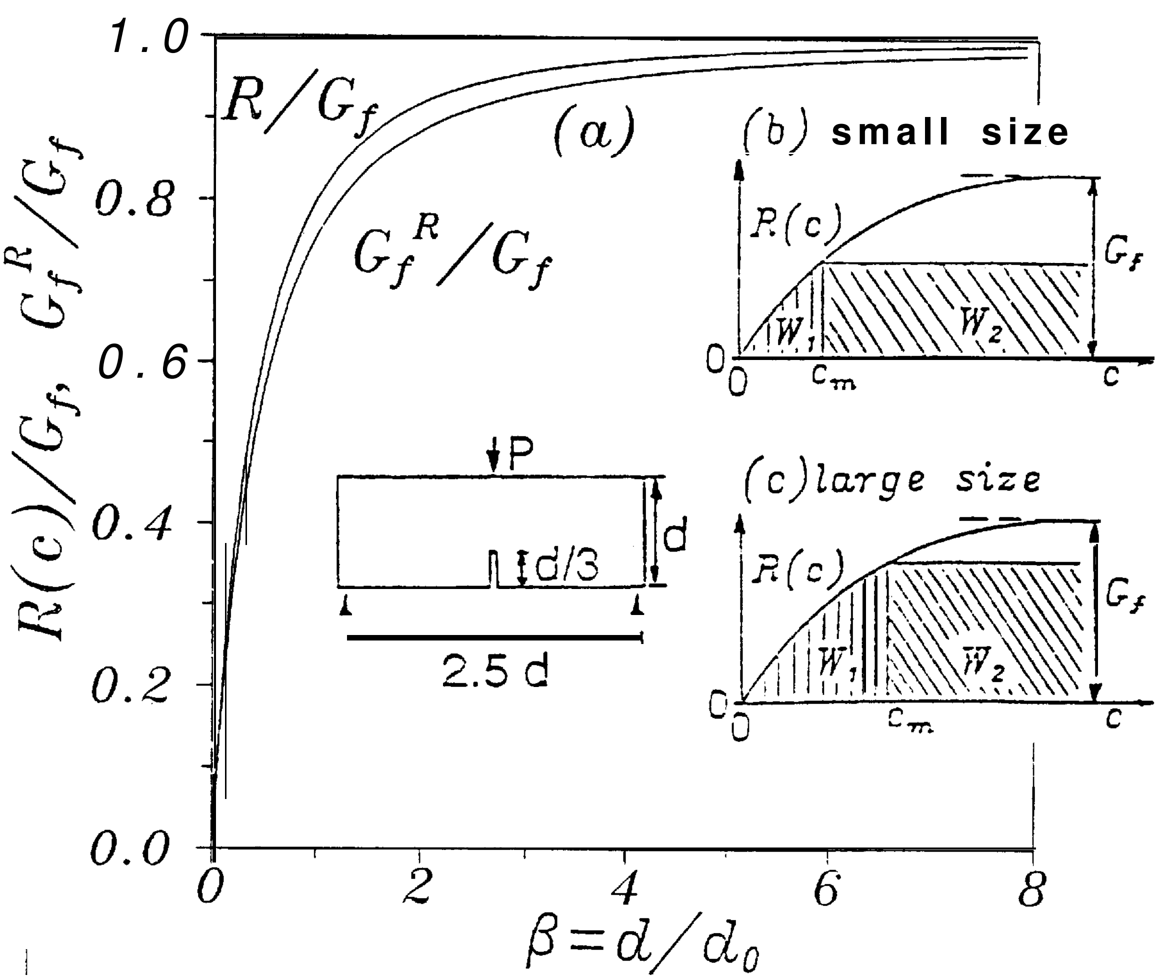

Fig.6.9 Theoretical Size Dependence of RILEM Fracture Energy G_f^R